SAE TECHNICAL PAPER SERIES

2000-01-3062

An Investigation of Electric Motor Drive Characteristics for EV and HEV Propulsion Systems

Z. Rahman, M. Ehsani and K. L. Butler
Texas A&M University

Reprinted From: Future Engines (SP-1559)

The Engineering Society For Advancing Mobility Land Sea Air and Space®
INTERNATIONAL

2000 Future Transportation Technology Conference
Costa Mesa, California
August 21-23, 2000

ISSN 0148-7191

Printed in USA

2000-01-3062

An Investigation of Electric Motor Drive Characteristics for EV and HEV Propulsion Systems

Z. Rahman, M. Ehsani and K. L. Butler
Texas A&M University

ABSTRACT

The recent growing interest in electric vehicle (EV) and hybrid electric vehicle (HEV) demands for an efficient, reliable and economical motor drive for electric propulsion. However, searching for a suitable traction motor becomes quite involved when vehicle dynamics and system architecture are considered. This paper makes an in-depth investigation on two highly important traction motor characteristics, extended speed range-ability and energy efficiency, from vehicular system perspective. The influences of these two motor drive features on a pure EV, a post-transmission, and two pre-transmission parallel HEV with 20% and 50% hybridization are studied in this paper. Two EV-HEV software packages 'V-ELPH' developed by Texas A&M University and 'ADVISOR' from NREL are used for simulation purposes. Based on the results in this paper, a systematic method is developed regarding the selection of traction drives for EV and HEV propulsion systems.

INTRODUCTION

Selection of an appropriate traction motor for electric and hybrid propulsion systems is very important. The automobile industries, including the three major car manufacturers in the United States and other car manufacturers abroad, are actively looking for better motor drive systems for EV and HEV. But searching for the suitable machine format can be quite involved for a vehicular traction application where the overall machine operating point is not tightly defined. Some of the motor characteristics mentioned in past literature on EV/HEV research regarding the selection of electric traction motors are [1, 2]:

- Torque density,
- Inverter size,
- Extended speed range-ability,
- Energy efficiency,
- Safety and reliability,
- Thermal cooling, and
- Cost.

Among the above-mentioned motor drive features, the extended speed range-ability and energy efficiency are the two basic characteristics that are influenced by vehicle dynamics and system architecture. Therefore, the selection of traction drives for particular vehicle architecture (EV, series and parallel HEV, etc.) demands special attention on the extended speed range-ability and energy efficiency.

The issue of extended speed range is significant to a vehicle's acceleration performance which is a design criteria usually determined by user's demand. However, in real time driving, the vehicle rarely operates in extreme conditions (i.e. high speed and acceleration). Thus, the issue of energy efficiency of the system becomes important. The miles per gallon (mpg) fuel economy is dictated by the energy efficiency of the overall system. To ensure better mpg, the location of the best efficiency contour of the traction drive should coincide with its frequently operating regions. Therefore, if the best traction motor is desired for a specific EV or HEV architecture, both extended speed range-ability and energy efficiency issues should be simultaneously investigated.

In this paper, the maximum extended speed range-ability and energy efficiency of traction drives are explored and their relative significances to EV and HEV architectures are identified. The SAE J1711 partial charge test (PCT) [3] procedure is followed to investigate frequent operating points of the motor and the engine in parallel HEV systems. The federal urban driving schedules (FUDS) and federal highway driving schedules (FHDS) are taken as the standardized driving behavior. The EV-HEV software packages 'V-ELPH' [4] developed in Texas A&M University and 'ADVISOR' [5] from NREL are used for simulation purposes.

EXTENDED SPEED OPERATION

Vehicle dynamics requires extended-speed, constant-power operation from the propulsion system in order to meet the vehicle's operating constraints (e.g., initial acceleration and grade-ability) with minimum power. The EV-HEV research group of Texas A&M University pointed out a unique methodology of selecting the traction motor based on the capability of motor operation in the extended constant power region [6]. It was revealed that initial acceleration and grade condition could be met with minimum power rating if the power train can be operated mostly in the constant power region. Generating the optimal torque-speed profile through the vehicle's propulsion system is extremely important, because it reduces the cost by reducing the system power rating.

CASE I: EV AND SERIES HEV

In a general EV or series HEV system, there is only one propulsion unit, which is the electric motor. The ideal force-speed profile of an electric motor is shown figure 1. This typical drive characteristic can be divided into two distinct sections: constant torque (or force) region and constant power region. In constant torque region the electric motor provides its constant rated torque 'T_{max}' (or F_{max}) up to its base speed 'N_b' (or v_{rm}). At this speed the motor reaches its rated power limit 'P_m'. The operation beyond the base speed is called constant power region. In this region the motor provides rated power up to its maximum speed. This is obtained by reducing the field flux of the motor and, therefore, is also known as 'field-weakening region'. Figure 1 denotes a '3.3x' type motor, where the constant power region extends beyond the constant torque region by a factor 3.3 (v_{max}/v_{rm}).

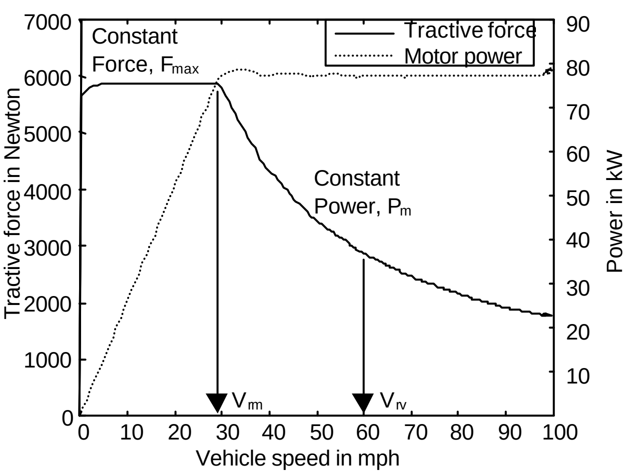

Figure 1. An ideal motor drive characteristics.

To calculate the total traction power of a vehicle, the constraint commonly imposed on the propulsion unit is the initial acceleration. The basic objective is to meet the acceleration performance with minimum power. An analytical expression relating traction power 'P_m' with initial acceleration (0 to v_{rv} mph in t_f seconds) is given in equation (1) where aerodynamic resistance and friction is neglected for the time being [6].

$$P_m = \frac{m}{2t_f}(v_{rm}^2 + v_{rv}^2) \quad (1)$$

$$\text{or, } F_{max} \cdot v_{rm} = \frac{m}{2t_f}(v_{rm}^2 + v_{rv}^2) \quad (2)$$

Here, m is vehicle mass in kg. The maximum force 'F_{max}' that a tire can handle without 'peeling out' or slipping limits the drive torque supplied by the power train. 'F_{max}' is calculated from equation (3).

$$F_{max} = \frac{\mu m g (L_2 + f_r h_g) / L}{1 + \mu h_g / L} \quad (3)$$

Here, f_r is coefficient of tire rolling resistance, μ is maximum wheel slip coefficient, h_g is the height of vehicle center of gravity from ground, L is vehicle wheel base and L_2 is horizontal distance of rear wheel from the center of gravity (see figure 2). In the above equations, (2) defines the acceleration power of the drive train and (3) imposes a limit on maximum traction force because of tire slipping. Eliminating 'F_{max}' and solving (2) and (3) we get equation (4).

$$v_{rm}^2 - \frac{2t_f (L + \mu h_g)}{\mu g (L_2 + f_r h_g)} v_{rm} + v_{rv}^2 = 0 \quad (4)$$

The quadratic form in equation (4) suggests two solutions for motor rated speed 'v_{rm}'. However, one value will be impractical. This implies that there exists a unique solution of maximum extended speed ratio for EV and the result is independent of vehicle weight.

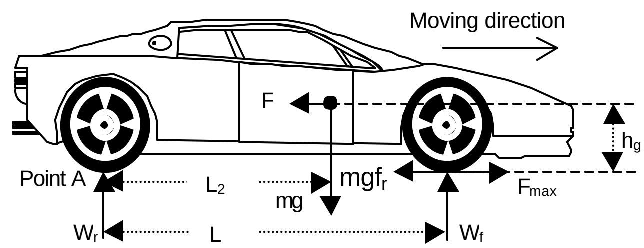

Figure 2. A summary of forces on a car.

For the work discussed in this paper, the resistance less case was considered. The Inclusion of aerodynamic drag and friction in equation (1) will result a complex form as shown below [6].

$$\int_0^{v_{rm}} \frac{m\,dv}{F_{max} - mgf_r - \frac{1}{2}\rho C_d A_f v^2} + \int_{v_{rm}}^{v_{rv}} \frac{m\,dv}{\frac{F_{max} \cdot v_{rm}}{v} - mgf_r - \frac{1}{2}\rho C_d A_f v^2} = t_f \quad (5)$$

Here, ρ is air density, C_d is aerodynamic drag coefficient, and A_f is the car's frontal area. Equation (5) is solvable by numerical integration. A detail description on how to get the maximum extended speed ratio using equations (3) and (5) is given in reference 7. The results obtained from numerical integration for the maximum extended speed range of a 1000 kg, 1600 kg and 2000 kg passenger car are presented in figure 3. The required initial acceleration considered in this example is 60 mph (v_{rv}=26.82 m/s) from standstill in 10 seconds (t_f=10 sec.) and, maximum cruising speed is assumed 100 mph. Necessary parametric description of the vehicle is presented in the appendix.

Figure 3 shows that the extended speed ratio (v_{rm}/v_{max}) is almost independent of vehicle mass. This is because aerodynamic drag, which is not a function of weight, has less impact on the extended speed ratio than the tire friction, which is a linear function of weight. Therefore, for a certain vehicle size the maximum extended speed ratio is unique and, in this example it is (100/19.2) 5.2x.

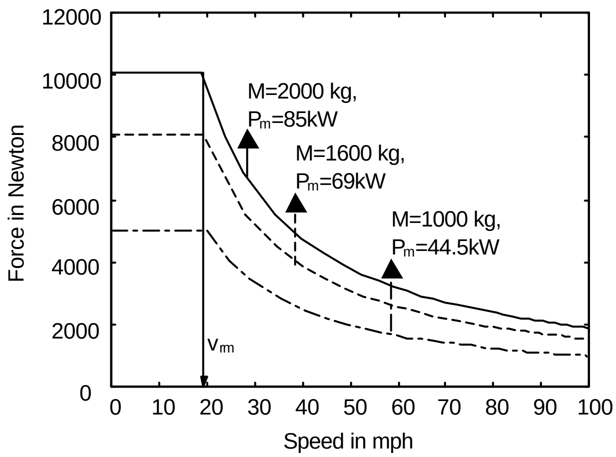

Figure 3. Maximum extended speed range of EV/series HEV.

CASE II: CONVENTIONAL CARS

Although equations (1), (2) and (5) were obtained for a pure electric propulsion system, the conception of extended speed operation still holds good for conventional internal combustion engine (ICE)-based vehicles. In engine driven vehicles, constant power operation is attained through a multi-gear transmission system. In figure 4, we observe a 90 kW engine achieving the ideal force-speed profile of a drive system using a 5-gear transmission. The gear ratios are 13.45, 7.57, 5.01, 3.77 and 2.84. The engine is modeled by linearly scaling the torque axis of a 102 kW spark ignition Dodge Caravan engine [5].

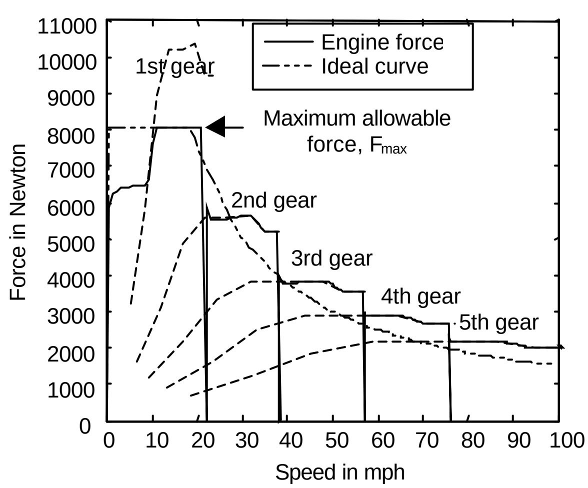

Figure 4. Conventional vehicle achieving the optimal force-speed profile with 5-gear transmission system.

CASE III: PARALLEL HEV

In parallel hybrid either the electric motor or engine or even both can propel the vehicle. Therefore, use of multi-gear transmission becomes necessary in parallel HEV because of the engine. Depending on the position of the transmission system there can be two parallel HEV architectures: pre-transmission and post-transmission hybrids. In pre-transmission hybrid (figure 5.a) the gearbox is on the main drive shaft and before the torque coupler. Therefore, the gearbox affects the performance of both engine and electric drive. In post-transmission hybrid (figure 5.b), the gearbox is on the engine shaft and after the torque coupler. Therefore, only the engine performance is affected by the gearbox. The electric drive may function on single gear speed reducer. This demands extended speed operation from the motor.

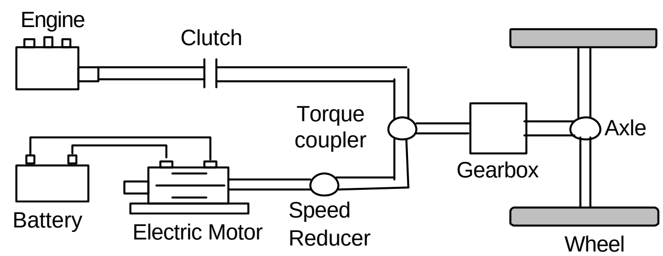

Figure 5.a. The pre-transmission architecture.

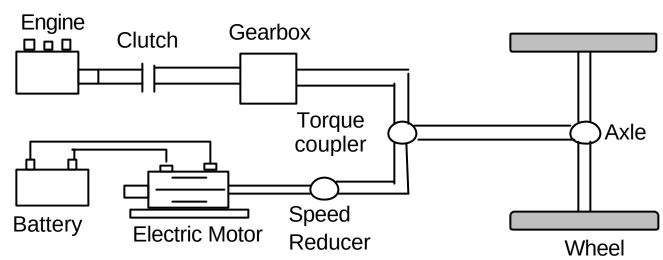

Figure 5.b. The post-transmission architecture.

<u>Post transmission HEV</u>

In a post-transmission hybrid system the extended speed ratio depends on the 'hybridization factor' (HF). This is the ratio between motor power and the total propulsion power 'P_{Total}', and is expressed in percentage ($HF=100\%\times P_m/P_{Total}$). Performance of the parallel HEV depends on HF. Increased HF means increased motor power. Since the electric motor is naturally more efficient than the ICE, increased HF will increase the overall system efficiency. However, the weight of the power train increases with increased hybridization. We carried out a detailed analysis on the performance of pre-transmission and post-transmission hybrid system with different HFs [8]. We concluded that a 50% HF gives the best fuel economy and also passes the SAE J1711 partial charge test (PCT). A parallel HEV over 50% hybridization failed to meet the charge sustainability criteria during PCT because a small sized engine fails to recharge the large battery pack during PCT in high hybridization. However, automobile industries favor lower HF because of their present ICE-based infrastructure which is reflected in trend of 20% HF observed in recently developed parallel hybrids [9, 10]. Therefore, in this paper we focus on parallel HEVs with 20% and 50% hybridization only.

The decrease in HF means decrease in motor power 'P_m'. This will effect equation (1). Therefore, the 'constant power' curve will shift downwards (see figure 6). But HF does not change the maximum force 'F_{max}' of the tire in equation (3). Thus, decreased hybridization means increase in extended speed ratio. Figure 6 illustrates the statement for a 1600 kg parallel HEV. A post-transmission hybrid system with 50% hybridization requires 2 times more of the maximum extended speed operation from the motor, which is (5.2÷0.5=) 10.4x. A 20% hybridized system requires (5.2÷0.2=) 26x. But no motor can provide such an extended speed range with a single gear. This indicates the necessity of using a separate multi-gear transmission with the motor drive in post-transmission parallel HEV.

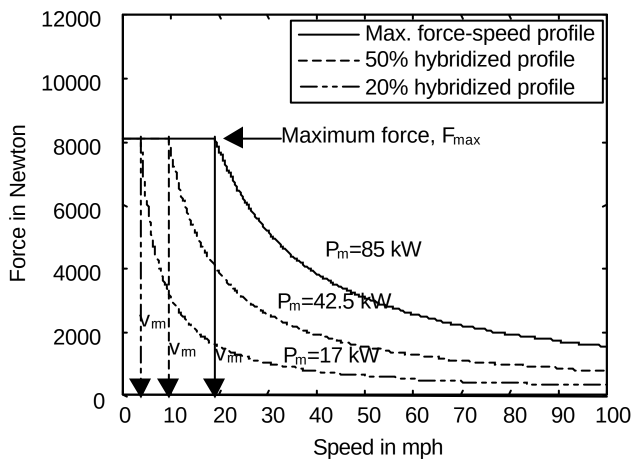

Figure 6. Extended speed range for post-transmission parallel HEV.

<u>Pre transmission HEV</u>

The maximum constant power range of the pre-transmission system is influenced by two factors: HF and transmission gears. The single gear speed reducer (see figure 5.b) equalizes maximum motor speed with maximum engine speed. The gearbox divides the entire force-speed profile of the vehicle into small sections (see figure 4). In these sections, the gear ratio decreases with increased gear number. The traction force decreases and speed increases proportionally with the decrease in gear ratio. But there is no change in power and in extended speed ratio (v_{max}/v_{rm}). Therefore, extended speed range should be looked at only in the 1st gear region where the applied traction force is maximum and limited by tire peeling. Figure 7.a shows the force-speed profile of a 45 kW motor matching with a 45 kW engine in a combined 90 kW (50% hybridization) pre-transmission hybrid operating in 1st gear ratio of 13.45. The maximum extended speed ratio of 2x is observed. Figure 7.b shows the force-speed profile of an 18 kW motor matching with a 72 kW engine in a combined 90 kW (20% hybridization) pre-transmission hybrid operating in 1st gear ratio of 13.45. In this case the maximum extended speed ratio is 5x.

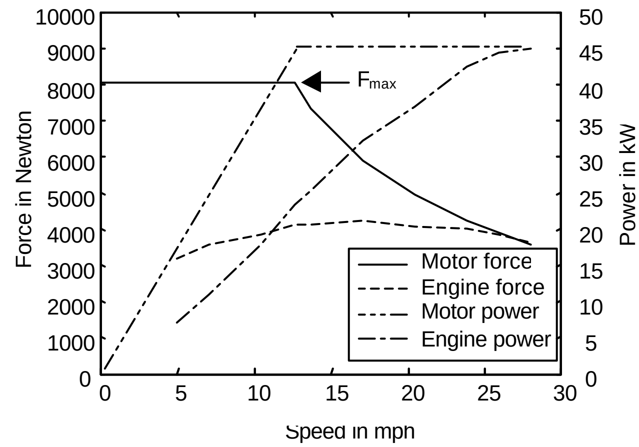

Figure 7.a. The force-speed profile of engine and motor of a 50% hybridized pre-transmission system shown in 1st gear operation.

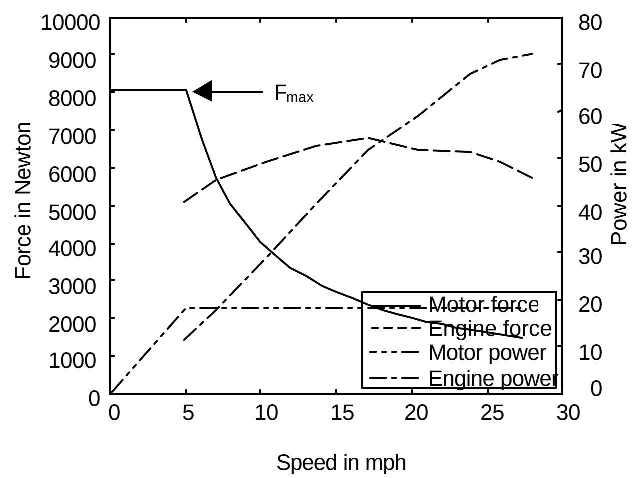

Figure 7.b. The force-speed profile of engine and motor of a 20% hybridized pre-transmission system shown in 1st gear operation.

ENERGY EFFICIENCY

Along with the suitable force vs. speed profile it is also essential to have a traction motor with high efficiency performance over a broad operating range. Standard industrial motors work in a certain operating point and the drive efficiency is defined at that point. A motor drive with a high efficiency in one operating point may not necessarily be efficient at all operating points. A traction motor needs to have a reasonable efficiency over its entire torque-speed profile. However, it is very difficult to design a motor that has high efficiency over its entire torque-speed profile. Thus, we propose to optimize its efficiency over its frequently operating region. We refer to this as 'energy efficiency' because efficiency is now also time dependent.

The two commonly accepted driving schedules to measure fuel economy of a car are FUDS and FHDS.

The overall fuel economy is calculated by weighing mpg from FUDS and FHDS with 0.55 and 0.45, respectively, and sum the results. In this paper, the frequent operating region of a traction motor is identified using FUDS and FHDS.

CASE I: EV AND SERIES HEV

The presence of a single propulsion unit makes the investigation of frequently operating region pretty straight forward in EV and series HEV. Figures 8.a and 8.b show the distribution of working points of a 1600 kg car for FUDS and FHDS. The figures show that the frequency of operation for FUDS is crowded in the low force (F<3000 Newton), low-medium speed (between 20 and 40 mph) region. For the FHDS drive cycle, the crowded region of operating points is between 40 to 60 mph. If we overlap the maximum force-speed profile of a 1600 kg EV/series HEV, given in figure 2, over figure 8.a and 8.b, it shows that when single gear is used the frequent operating regions of FUDS and FHDS are located in the constant power region of the motor. Therefore, with single gear operation, a traction motor that is highly efficient in its constant power region is best suited for EV and series HEV application.

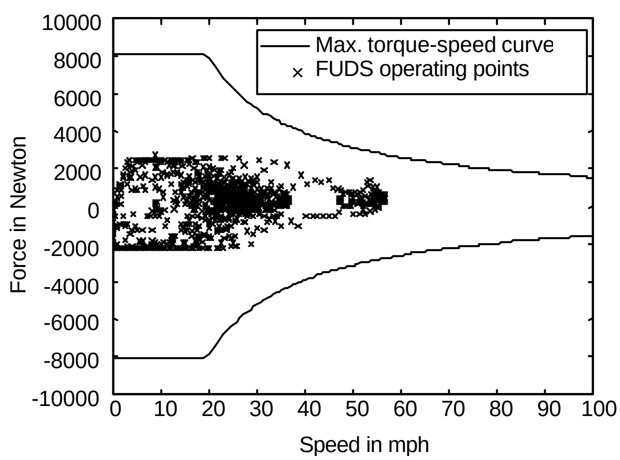

Figure 8.a. Distribution of working points of a 1600 kg car on FUDS.

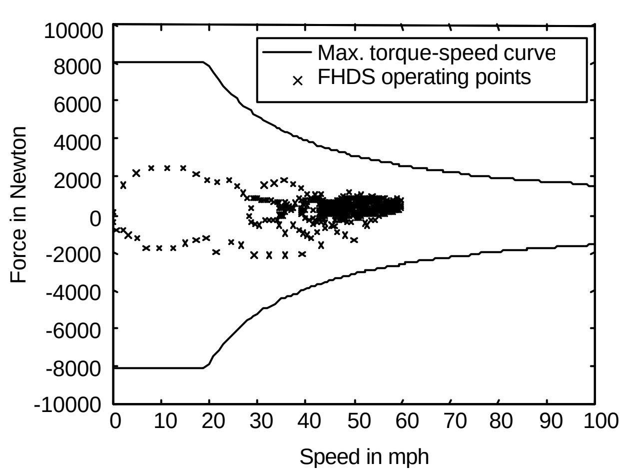

Figure 8.b. Distribution of working points of a 1600 kg car on FHDS.

CASE II: PARALLEL HEV

Figures 8.a and 8.b are applicable only to EV and series HEV where the only propulsion power comes from electric motor. Defining energy efficiency is very complex for parallel HEV in which degree of hybridization has a direct influence on the system. Furthermore, the polymorphism of parallel HEV architecture, like pre-transmission and post-transmission along with various power flow control concepts makes the efficiency study even more complicated. There are quite a few HEV control strategies mentioned in literature [5, 11-12]. The general idea of most of the power split algorithms are to maximize fuel economy by operating the two power sources in their better efficiency regions. Therefore, we would let the engine run in high-speed constant power region where it is more efficient than its other regions. On the other hand, the motor most of the time would operate on the low speed, high torque region where it is more efficient than the engine. Of course, the state of charge of the energy source pack also influences the control technique. In figures 9.a and 9.b, we present the frequency of operating points of the motor and engine for a 50% hybridized pre-transmission HEV on FUDS. Figure 10.a and 10.b shows the same on FHDS. The 'electrically assist' [5] control scheme was used for both cases. The force-speed characteristics of the motor and engine used in the simulations are given in figure 7.a. The propulsion forces in figure 7.a are converted to corresponding motor and engine torques in figures 9 and 10 assuming a wheel radius of 0.282m and, also considering 5-gear transmission ratios of 13.45, 7.57, 5.01, 3.77 and 2.84. The SAE J1711 PCT procedure is followed to ensure the charge sustainability of the HEV system. The two conditions maintained in our simulation settings are: (1) the energy packs are initially charged at 60% and, (2) after each driving schedule the difference between initial and final battery state of charge should be within 0.5%. We observe from figure 9.a and 10.a the frequent motor operating region in both cases are concentrated in the constant torque region of the motor. Therefore, traction motors used for a 50% hybridized parallel pre-transmission hybrid should maximize drive efficiency in the constant torque region.

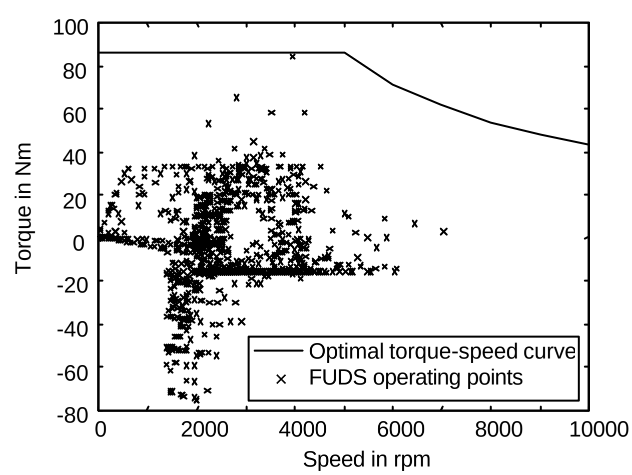

Figure 9.a. Distribution of motor operating points for a 50% pre-transmission HEV on FUDS.

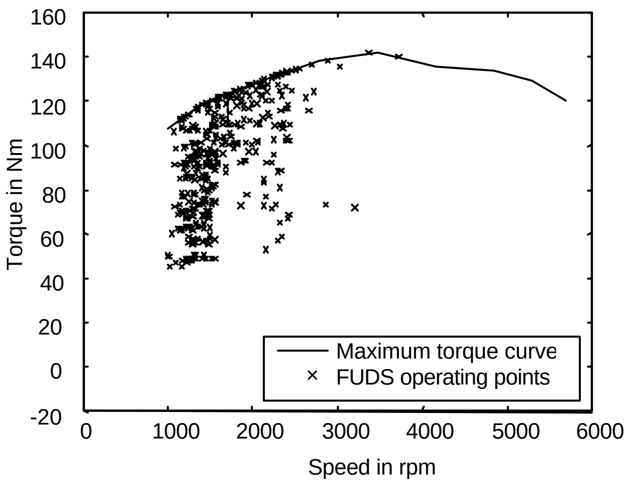

Figure 9.b. Distribution of engine operating points for a 50% pre-transmission HEV on FUDS.

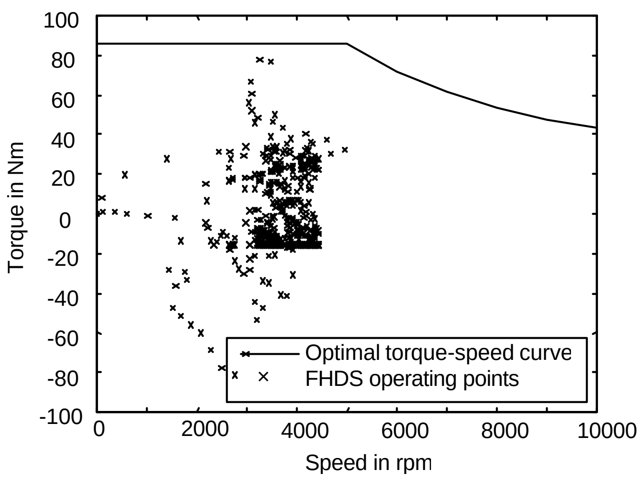

Figure 10.a. Distribution of motor operating points for a 50% pre-transmission HEV on FHDS.

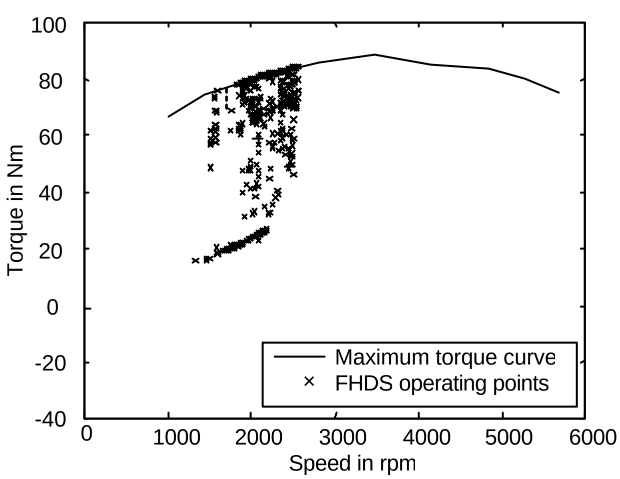

Figure 10.b. Distribution of engine operating points for a 50% pre-transmission HEV on FHDS.

A similar analysis is done for 20% hybridized parallel pre-transmission system as shown in figures 11 and 12. The force-speed characteristics of the motor and the engine used in the simulation are given in figure 7.b. Figure 11.a shows that the frequent motor operating region is just over 2000 rpm range, which is the beginning of the constant power region in this case. In figure 12.a the frequent motor operating region is clearly in the constant power region of the motor (just above 3000 rpm). Therefore, for a 20% hybridized parallel HEV system the traction motor efficiency should be maximized in the beginning of the constant power region.

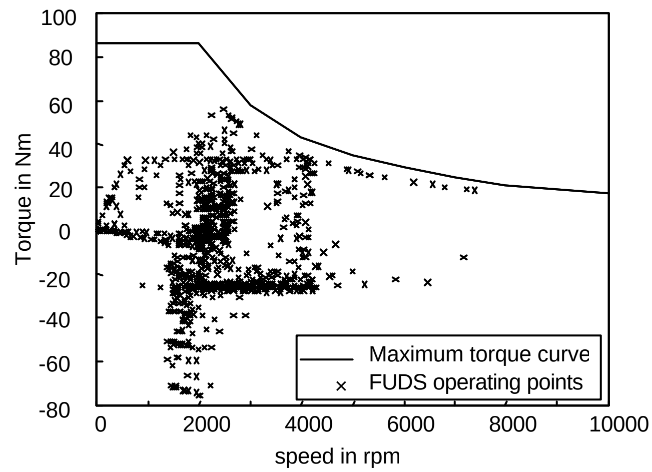

Figure 11.a. Distribution of motor operating points for a 20% pre-transmission HEV on FUDS.

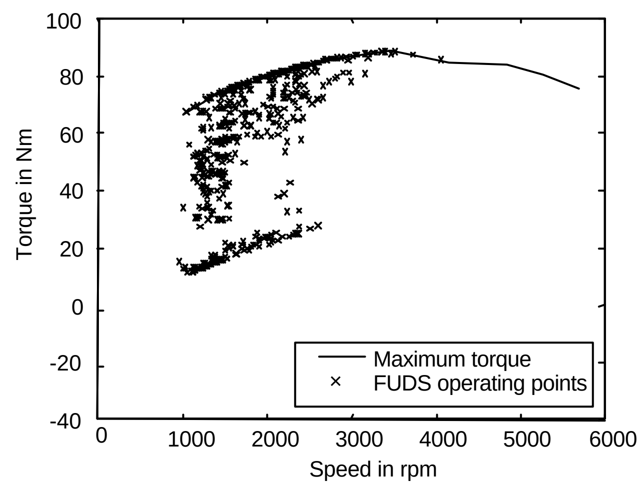

Figure 11.b. Distribution of engine operating points for a 20% pre-transmission HEV on FHDS.

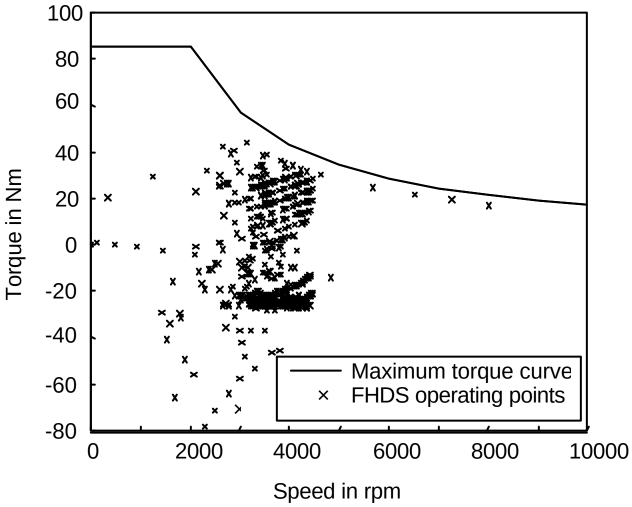

Figure 12.a. Distribution of motor operating points for a 20% pre-transmission HEV on FHDS

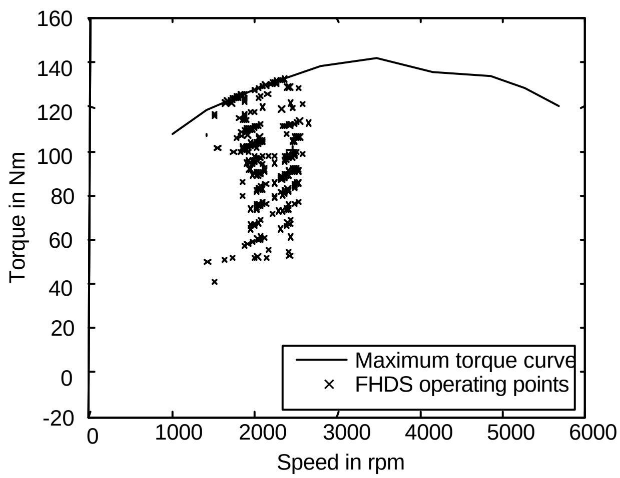

Figure 12.b. Distribution of engine operating points for a 20% pre-transmission HEV on FHDS.

MOTOR SELECTION ISSUES

Selection of traction motors requires special attention to their extended speed range-ability and efficiency contour. Some motor types have inherent property of operating with large extended speeds. The separately excited DC motor is an example. However, the principal problems of the DC motor are its commutators and brushes which limit the maximum speed of the motor, create sparks and require regular maintenance. Induction motor (IM) can achieve a large speed range with field-oriented control. The well-known technology and existing manufacturing infrastructure makes IM today's leading motor technology in EV-HEV application. However, the nonlinearity of the dynamic IM model and dependency on motor parameters make the control complex.

The switched reluctance motor (SRM) generates series-type torque-speed characteristics and has the ability to boost the torque above base speed by 'phase-advancing' [13]. This control technique is also nonlinear and machine dependent. A wide speed range of 6x in 1hp rating was reported in recent publication [14]. Therefore, SRM should be considered a serious candidate for EV, series HEV and low hybridized parallel HEV.

In the permanent magnet motor (PMM), the demagnetizing effect limits its wide speed range-ability. With an extended speed ratio of 2x, PMM can be a good candidate for 50% hybridized parallel HEV. However, cost, safety and cooling are other important issues relevant to PMM. Large magnets for high power PMM are expensive. The permanent field may cause severe consequence during short circuit faults. Also, magnets are sensitive to high temperature. Extra precautions need to be taken to keep the magnet cool, or else, motor efficiency drastically decreases. Demagnetization can also occur at 'Curie temperature'.

Regarding the energy efficiency issue, selection of an appropriate type of traction motor is very complicated. Motor efficiency is significantly influenced by material quality, design parameters and control technology. Again, the position of efficiency contours in the torque-speed map is also related to the type of motor. To investigate this, we focus on copper loss and iron loss, as they are the two dominating motor losses.

Copper loss is squarely proportional to the motor current. In IM and SRM, a portion of this current is also the motor magnetizing current, which produces magnetization or excitation loss. PMM is naturally excited through magnets and, therefore, has no excitation loss. However, this is only true below the base speed of the motor. Above the base speed, PMM requires external excitation to weaken its naturally existing magnetic field. Therefore, torque per copper loss is inherently better below the base speed in PMM.

IM and SRM suffer from excitation penalty below base speed. Excitation loss decreases above the base speed in IM as the 'field-weakening' method is done. Therefore, torque per copper losses improves above the base speed in IM. However, apart from the excitation loss, IM also has slip-dependent rotor copper loss. This creates the problem of heat attraction from the rotor core. In the case of SRM, excitation loss cannot be separately identified from copper loss. It was reported in past literature [14] that torque per ampere improves above the base speed in SRM. However, very little test data has been published in this regard.

At very high speed, iron loss becomes significant. Iron losses are a function of flux density and frequency of flux alternation. The PMM has rotor magnets. Therefore, it has theoretically zero rotor iron loss. The only iron loss in PMM is in the stator side. IM and SRM have both the stator and rotor iron losses. Harris and Miller predicted less iron loss in SRM compared to IM because of relatively low magnetic loading [13]. However, the variation of iron loss in SRM above and below base speed has not been studied in the past. We are currently investigating the pattern of efficiency contours in SRM.

Based on our preliminary studies on wide speed range-ability and energy efficiency, PMM is a suitable motor for a 50% hybridized car because of its superior efficiency in constant torque regime. However, for a 20% hybridized car, SRM may be a better choice for its extended speed range-ability and a sufficiently good efficiency (equal or better than IM) at constant power regime.

CONCLUSION

An in-depth analysis of two important drive characteristics, extended speed range-ability and energy efficiency, is presented in this paper. An analytical method of solving for maximum required extended speed ratio for EV and HEV architecture is presented. The sensitivity of the extended speed range to the level of hybridization is discussed. A fundamental method for selecting motor drives on the basis of energy efficiency is presented. Three types of traction motors, IM, SRM, and PMM are evaluated on the basis of extended speed and energy efficiency. The methodology discussed in the paper will be useful in the selection of traction motors for EV and HEV architectures where extended speed range and drive efficiency are the major selection criteria.

ACKOWLEGEMENT

The authors affirm their appreciation to all the students and faculty persons in the HEV research group of Texas A&M University in developing V-ELPH 2.01. Support for this work was provided by the Texas Higher Education Coordinating Board Advanced Technology Program (ATP) and the Office of the Vice President for Research and Associate Provost for Graduate Studies, through the Center for Energy and Mineral Resources, Texas A&M University, College Station.

CONTACT

Ziaur Rahman, Dr. Mehrdad Ehsani and Dr. Karen Butler can be reached through the Department of Electrical Engineering, Texas A&M University, College Station, Texas at (979)845-7441, or email zirhum@ee.tamu.edu, klbutler@ee.tamu.edu and ehsani@ee.tamu.edu.

APPENDIX

Vehicle parameters:

• Mass, m	1600 kg
• Height of CG, h_g	0.5 m
• Frontal area, A_f	2.04 m^2
• Wheel radius, r	0.282 m
• Wheel base, L	2.6 m
• Rear wheel from CG, L_2	1.56 m
• Wheel slip coefficient, μ	1.0212
• Rolling coefficient, f_r	0.009
• Air drag coefficient, C_d	0.33
• Single gear ratio, i_t	6.05

REFERENCE

1. K. M. Rahman, M. Ehsani, "Performance analysis of electric motor drives for electric and hybrid electric vehicle applications", *Power Electronics in Transportation, IEEE 1996, Page(s): 49 –56.*
2. N. Schofield, M. K. Jenkins, "High performance brushless permanent magnet traction drives for hybrid electric vehicles", *Machines and Drives for Electric and Hybrid Vehicles (Digest No: 1996/152), IEE Colloquium on 1996, Page(s): 4/1 -4/6.*
3. Electric Vehicle Forum Committee, "SAE J1711—Hybrid Electric Vehicle Emissions and Energy Consumption Test Procedure".
4. K. L. Butler, K. M. Stevens, M. Ehsani, "A versatile computer simulation tool for design and analysis of electric and hybrid drive trains", *SAE 970199*.
5. ADVISOR, *http://www.ctts.nrel.gov*.
6. M. Ehsani, K. M. Rahman, H. A. Toliyat, "Propulsion system design of electric and hybrid vehicles", *IEEE Trans. On Ind. Electronics, vol. 44, no. 1, pp. 19-27, Feb 1997.*
7. Z. Rahman, K. L. Butler, M. Ehsani, "Effect of extended-speed, constant-power operation of electric drives on the design and performance of EV-HEV propulsion system", *SAE 2000-01-1557*.
8. Z. Rahman, K. L. Butler, M. Ehsani, "A comparison study between two parallel hybrid control concepts", *SAE 2000-01-0994*.
9. W. Buschhaus, L. R. Brandenburg, R. M. Stuntz, "Hybrid electric vehicle development at Ford," *Proc. of 15th Elect. Veh. Symp. 1998*.
10. T. Kikuchi, H. Morita, E. Inada, T. Aso, "Evaluation tests of Nissan hybrid electric vehicle," *Proc. of 14th Elect. Veh. Symp. 1997*.
11. M. Ehsani, "Electrically Peaking Hybrid Systems and Method", *US Patent # 5,586,613, Dec. 1996*.
12. C. Hochgraf, M. Ryan and H. Weigman, "Engine control strategy for a series hybrid electric vehicle incorporating load-leveling and computer controlled management", *SAE 960230.*
13. T. J. E. Miller, "Switched Reluctance Motors and Their Control", *Magna Physics publishing division, Jan. 1993, Page: 145.*
14. K. M. Rahman, B. Fahimi, G. Suresh, A. V. Rajarathnam, M. Ehsani, "Advantages of switched reluctance motor applications to EV and HEV: design and control issues", *IEEE Trans. on Ind. Application, vol. 36, Issue 1, pp. 111 – 121, Jan/Feb 2000.*